Habitat compression and expansion of sea urchins in response to changing climate conditions on the California continental shelf and slope (1994–2013)

Kirk N. Sato [a,*], Lisa A. Levin [a], Kenneth Schiff [b]

[a] Center for Marine Biodiversity and Conservation, Scripps Institution of Oceanography, University of California, San Diego, 9500 Gilman Dr., La Jolla, CA 92093-0218, United States
[b] Southern California Coastal Water Research Project, 3535 Harbor Blvd., Costa Mesa, CA 92626, United States

A B S T R A C T

Echinoid sea urchins with distributions along the continental shelf and slope of the eastern Pacific often dominate the megafauna community. This occurs despite their exposure to naturally low dissolved oxygen (DO) waters ($< 60 \, \mu mol \, kg^{-1}$) associated with the Oxygen Limited Zone and low-pH waters undersaturated with respect to calcium carbonate ($\Omega_{CaCO3} < 1$). Here we present vertical depth distribution and density analyses of historical otter trawl data collected in the Southern California Bight (SCB) from 1994 to 2013 to address the question: Do changes in echinoid density and species' depth distributions along the continental margin in the SCB reflect observed secular or interannual changes in climate? Deep-dwelling burrowing urchins (*Brissopsis pacifica*, *Brisaster* spp. and *Spatangus californicus*), which are adapted to low-DO, low-pH conditions appeared to have expanded their vertical distributions and populations upslope over the past decade (2003–2013), and densities of the deep pink urchin, *Strongylocentrotus fragilis*, increased significantly in the upper 500 m of the SCB. Conversely, the shallower urchin, *Lytechinus pictus*, exhibited depth shoaling and density decreases within the upper 200 m of the SCB from 1994 to 2013. Oxygen and pH in the SCB also vary inter-annually due to varying strengths of the El Niño Southern Oscillation (ENSO). Changes in depth distributions and densities were correlated with bi-monthly ENSO climate indices in the region. Our results suggest that both a secular trend in ocean deoxygenation and acidification and varying strength of ENSO may be linked to echinoid species distributions and densities, creating habitat compression in some and habitat expansion in others. Potential life-history mechanisms underlying depth and density changes observed over these time periods include migration, mortality, and recruitment. These types of analyses are needed for a broad suite of benthic species in order to identify and manage climate-sensitive species on the margin.

© 2016 Published by Elsevier Ltd.

1. Introduction

Continental margin ecosystems in eastern boundary upwelling regions such as the west coast of North America experience dynamic natural variations in biogeochemical cycles on various spatiotemporal scales. Oscillations in ocean-atmosphere coupled processes occur naturally on millennial (Moffitt et al., 2015), decadal (Mantua et al., 1997), and interannual (Bjerknes, 1966) time-scales; these can have basin-wide effects on population dynamics and global climate change variables such as seawater pH, dissolved oxygen (DO), and temperature (reviewed in Levin et al., 2015). The

Southern California Bight (SCB) is a 700-km long region influenced by the upwelling of cold, nutrient-rich, deep water characterized by relatively low DO, low pH, and high carbon dioxide (CO_2). Benthic and epibenthic organisms may already be functioning at their physiological limits at the seawater-seafloor interface where the continental slope intersects with a permanent dissolved Oxygen Minimum Zone (OMZ) and Carbon Maximum Zone (Paulmier et al., 2011), therefore making these regions particular 'hotspots' of future climate change (Gruber, 2011).

Oxygen Limited Zones (OLZs) are the regions above and beneath the OMZ where DO concentrations of $< 60 \, \mu mol \, kg^{-1}$ are often considered hypoxic habitat for marine organisms (Gilly et al., 2013), although this threshold may not be relevant for organisms with very low metabolic oxygen demands (Seibel, 2011; Somero et al., 2016). Time-series analysis from 1984 to 2006 of quarterly cruise data in the SCB collected by the

* Corresponding author.
  E-mail addresses: knsato@ucsd.edu (K.N. Sato), llevin@ucsd.edu (L.A. Levin), kens@sccwrp.org (K. Schiff).

2   K.N. Sato et al. / Deep-Sea Research II ∎ (∎∎∎∎) ∎∎∎–∎∎∎

California Cooperative Ocean Fisheries Investigations (CalCOFI) reveal oxygen declines, with an average decrease in DO of $\sim 1\ \mu mol\ kg^{-1}\ yr^{-1}$ at 200-m stations and a shoaling of the OLZ boundary of $> 80\ m$ at some inshore stations (Bograd et al., 2008). An updated analysis of these data (1984–2010) showed a decrease of $0.76\ \mu mol\ kg^{-1}\ yr^{-1}$ at the $25.8\ kg\ m^{-3}$ isopycnal (Bograd et al., 2015). Due to microbially-mediated remineralization processes, similar reductions in pH and increases in pCO_2 are expected to have accompanied the expansion of low oxygen zones in the SCB (Gilly et al., 2013; Gruber, 2011; Paulmier et al., 2011; Reum et al., 2016). Seawater pH and DO are strongly correlated in nearshore kelp forests (Frieder et al., 2012) and in the deep sea (Alin et al., 2012; Nam et al., 2015). In addition, secular increases in nutrient concentrations and chlorophyll a have been observed from the same CalCOFI dataset (Bograd et al., 2015). One potential mechanism for shoaling hypoxia and changes in nutrients in the SCB include a strengthening of the CA Undercurrent, which originates from subtropical equatorial water from the south and is characterized by relatively warm, high saline, low DO, and low pH water (Bograd et al., 2015).

Koslow et al. (2011) reported striking shifts in mesopelagic and demersal larval fish community structure accompanying these decadal changes in midwater DO. Twenty four of 27 larval fish taxa collected by seasonal CalCOFI cruises demonstrated a strong relationship with midwater DO and multiple climate indices such as the Pacific Decadal Oscillation (PDO), El Niño Southern Oscillation (ENSO), and the North Pacific Gyre Oscillation (NPGO) (Koslow et al., 2011, 2015). Although the CalCOFI biological time-series provides extensive spatial and temporal coverage of pelagic species, the interactions of benthic faunal populations with climate variability along the SCB continental margin have been understudied. The phenomenon of vertical habitat compression in the ocean due to shoaling hypoxia was hypothesized to negatively affect aerobic groundfish (McClatchie et al., 2010) and mesopelagic fish (Netburn and Koslow, 2015) in southern CA and billfish in the Eastern Tropical Pacific (Prince and Goodyear, 2006; Stramma et al., 2012). However, few datasets exist to assess trends in megafauna species populations that dominant the benthos such as echinoids in the SCB (Keller et al., 2012).

Beyond the longer-term changes in oxygenation and likely pH and pCO_2, the SCB is highly dynamic on interannual, seasonal, and even diurnal and semidiurnal time scales (Nam et al., 2015; Booth et al., 2012; Send and Nam, 2012). For example, during El Niño events, elevated temperatures and reduced upwelling lead to low productivity, less respiration and biogeochemical drawdown, thus higher oxygen levels (Ito and Deutsch, 2013), while the opposite occurs during La Niña events (Nam et al., 2011). Over the last 25 years, the Multivariate ENSO Index (MEI), a composite of six key ocean-atmospheric variables: sea-level pressure, zonal and meridional components of the surface wind, sea surface temperature, surface air temperature, and total cloudiness (Wolter and Timlin, 2011), indicates a range of El Niño and La Niña strengths occurring in the Pacific Ocean, including one exceedingly strong El Niño in 1997–1998 (Fig. 1). Nam et al. (2011) advise caution when extrapolating their correlation results from a single El Niño-La Niña cycle to other ENSO indices, and few studies examined the direct relationship between ENSO and dissolved oxygen (see Arntz et al., 2006) despite the abundance of historical cruise data and the potentially important ecological implications (McClatchie, 2014).

Echinoderms are important benthic fauna ecologically; they are often identified as ecosystem engineers and in some cases, keystone predators or grazers (Paine, 1966). Biocalcification by echinoderms (e.g. sea urchins, sea stars, cucumbers, brittle stars, crinoids) contributes to globally significant carbon production rates that may rival production rates of coral reefs (Lebrato et al., 2010),

and are surprisingly tolerant to low carbonate saturation states (Lebrato et al., 2016).

In the SCB, multiple deep-dwelling sea urchin species are abundant over broad depth ranges (Thompson et al., 1993) characterized by sharp gradients in oxygen, pH, and Ω (saturation state) levels that are comparable to or much lower than future ocean acidification and deoxygenation scenarios predicted for the surface ocean (Alin et al., 2012; Levin and Dayton, 2009; Nam et al., 2015). Experiments suggest that multiple life-history stages of calcifying benthic organisms, including echinoid urchins, will respond negatively to ocean acidification and hypoxia conditions (Dupont et al., 2010; Frieder, 2014; Kroeker et al., 2013). The vast majority of these studies have been conducted on shallow-water species however, and the response of deep-margin species to deoxygenation, ocean acidification, and calcium carbonate saturation ($\Omega_{CaCO_3} = 1$) reduction is poorly understood (Barry et al., 2014; Hofmann et al., 2010; Taylor et al., 2014).

Detecting faunal response to long-term environmental change requires time-series sampling (Glover et al., 2010). The Southern California Coastal Water Research Project (SCCWRP) is a collaborative inter-agency environmental monitoring program that makes publicly available a time-series dataset of georeferenced benthic and epibenthic megafauna community data in southern California along the continental shelf and slope. The SCCWRP otter trawl surveys of the SCB shelf and slope benthos have occurred every 4–5 years since 1994 to water depths of 200 m, providing 5 time points in order to assess population trends in benthic fauna. In 2003 the SCCWRP *Bight* program extended their sampling depths down to 500 m, providing only 3 survey time points to the present, but extending spatial coverage into deep waters. These fishery-independent data provide a unique suite of multi-decadal samples that can be used to address questions about benthic community changes over time in the SCB.

The objective of this study was to investigate temporal changes in (1) depth distributions and (2) density estimates of five continental margin sea urchin species throughout the SCB from 1994 to 2013 to better understand echinoid response to environmental change. We hypothesized that various depth distribution parameters of deeper-occurring urchin species, which are tolerant to low oxygen, high CO_2 conditions in the upper OMZ (Helly and Levin, 2004) and OLZ (Gilly et al., 2013) would exhibit evidence of habitat expansion consistent with observed shoaling oxyclines in the region (Bograd et al., 2015; Bograd et al., 2008). This secular trend would suggest that these species have expanded their distribution into shallower waters enabled by a combination of environmental adaptation and ecological interactions. Urchin species with shallower distributions were hypothesized to be more vulnerable to expanding OMZ conditions and to have experienced habitat compression over this time period. In addition, we hypothesized that the density of shallower-occurring urchins would decrease in the upper 200 m from 1994 to 2013 due to the shoaling and intensification of hypoxic waters, and the density of deeper-occurring urchins in the upper 500 m would increase from 2003 to 2013 due to migration from deeper depths as habitat compression excludes shallower competitors. Alternatively, these trends could also be driven by environmental factors other than oxygen that may co-vary with time, such as changes in dissolved CO_2, food, temperature, and ecological interactions. Chlorophyll a concentration in the SCB has increased over recent decades (Bograd et al., 2015) and could lead to more food and higher densities in all species over time. In contrast, El Niño conditions, which occurred in 1997–1998 and 2002–2003 are associated with higher oxygenation and lower phytoplankton and kelp production (Ito and Deutsch, 2013), and should produce an opposite response to that expected from expanding OMZs. We
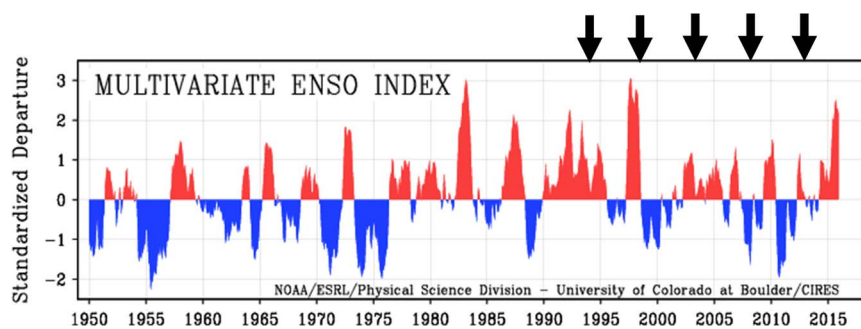
Fig. 1. Figure modified from http://www.esrl.noaa.gov/psd/enso/mei/. Time-series of MEI with black arrows indicating years when trawl surveys occurred throughout the Southern California Bight. Negative values of the MEI (blue) represent the cold ENSO phase (La Niña). Positive MEI values (red) represent the warm ENSO phase (El Niño). (For interpretation of the references to color in this figure legend, the reader is referred to the web version of this article.)
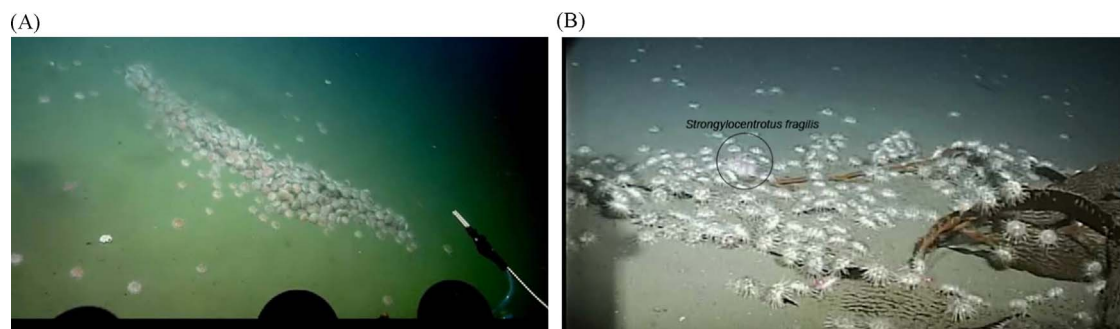
(A) (B)

Fig. 2. A. Aggregation of pink urchins (*Strongylocentrotus fragilis*) in the OLZ (~400 m) off of San Diego, CA. Remotely operated vehicle (ROV) footage courtesy: R/V *Nautilus*, NOAA, cruise ID NA066. B. Feeding aggregation of white urchins (*Lytechinus pictus*) on giant kelp (*Macrocystis pyrifera*) at ~100 m depth off the coast of La Jolla, CA. Presence of individual *S. fragilis* (circled) suggests these species compete for kelp resources at this depth. ROV footage courtesy: Scripps Institution of Oceanography, cruise ID MV1217.

hypothesized a deepening of hypoxia-intolerant species and possibly lower densities of all species in response to El Niño.

2. Materials and methods

We analyzed biological benthic survey data collected along the continental shelf and slope in the SCB. Depth distributions of shelf and slope sea urchins in the upper 200 and upper 500 m were determined for each survey year for five species of echinoderm echinoids: the white urchin (*Lytechinus pictus*), the pink urchin (*Strongylocentrotus fragilis*), and three burrowing urchins (*Brissopsis pacifica*, *Brisaster* spp. and *Spatangus californicus*). *Brisaster townsendi* and *B. latifrons* were grouped together as their ranges overlap in the SCB (Hood and Mooi, 1998) and they were often reported as *Brisaster* spp. in the field. Site-specific counts were standardized to obtain population density (count m^{-2}) for each sea urchin species and were compared among survey years and depth bins.

2.1. Data collection: trawl program and counts

The megafauna community was sampled at randomized stations by otter trawl across the SCB by trained taxonomists during the summer months (July–September) of years in which the Bight program was conducted (1994, 1998, 2003, 2008 and 2013) with 7.6 m head-rope semiballoon otter trawl nets fitted with 1.25-cm cod-end mesh. Trawls were towed along open-coast isobaths for ~10 min at 1.5–2.0 nautical miles per hour during daylight hours. Trawl distance was calculated from the start and stop fishing GPS coordinates, which acted as a proxy for the net's relative position. It was assumed the net remained on the bottom and was fishing the entire time. *S. fragilis* and *L. pictus* often form feeding aggregations on kelp falls (Sato and Levin, *personal observation*; Fig. 2A, B), which

may bias density estimates, but the high number of trawls conducted each survey year is likely to capture this variability. One exception where kelp falls have been found to be more abundant is in submarine canyons (Harrold et al., 1998), but sites were surveyed for flat, trawlable ground prior to net deployment and sites in canyons were avoided. Upon retrieval, catches were sorted, identified to species, and enumerated. Each station was sampled once per survey (Fig. 3). Bay sites and sites at water depths < 10 m were removed from this analysis in order to minimize zero inflated data (Thompson et al., 1993). Only echinoid data representing 5 species are reported here.

2.2. Evaluation of area sampled and density estimates

The area swept by each trawl was calculated as the distance trawled (m) x 4.9 m (the width of the trawl) (*sensu* Miller and Schiff, 2012). Densities obtained per trawl were determined for each of the 5 urchin species for each survey year by dividing the species count by the area swept. Density means were also calculated for 50-m and 100-m depth bins in addition to 10–200 m (1994–2013 survey time period) and 10–500 m (2003–2013 surveys) depth bins.

2.3. Species distribution in the SCB

The start depths of each trawl station were recorded to the nearest meter on board survey vessels; trawls were made along depth contours so the start depth reflected the actual depth of the trawl. All individuals of each species were assigned the start depth of the trawl from which they were collected. Depth distributions of trawls containing one or more individuals were determined for each species for each survey year. For each species, trawls that contained one or more individuals were separated, and the upper and lower depth limits, the mean depth, and the first and third
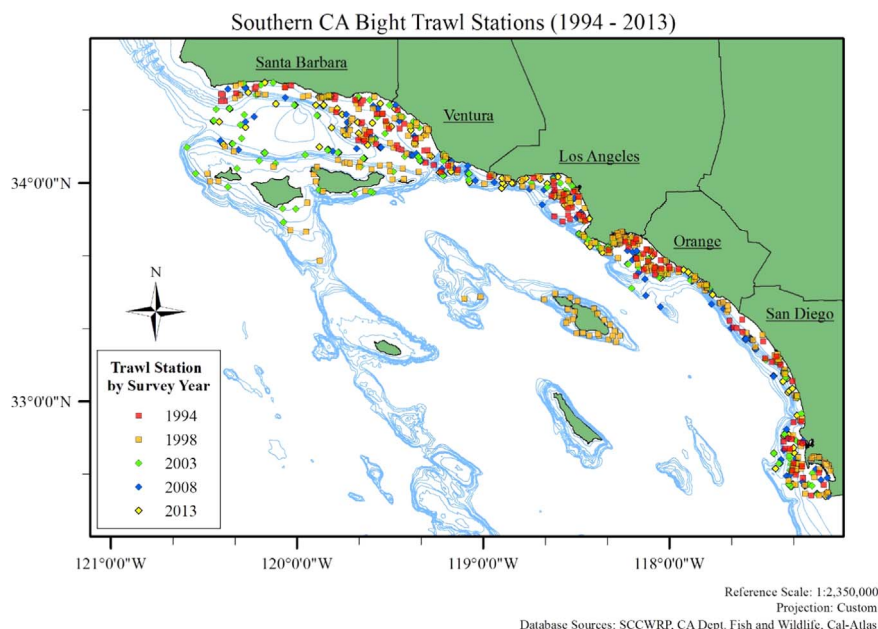
Fig. 3. Map of otter trawl survey stations from 1994 to 2013 in the Southern California Bight (SCCWRP). Black lines indicate boundaries between California counties (green) (Cal-Atlas, http://atlas.ca.gov/download.html#/). Ocean depth contours (light blue lines) are marked every 50-m starting at 50 m and extending to 500 m (CA Department of Fish and Wildlife, ftp://ftp.dfg.ca.gov/R7_MR/BATHYMETRY/). Diamond symbols indicate stations between 10 m and 500 m used for every urchin species during 2003 (light green), 2008 (blue), and 2013 (yellow) surveys. Square symbols indicate stations between 10 m and 200 m used in *L. pictus* analyses for 1994 (red) and 1998 (orange) surveys. Map created using ArcMap™ v.10.1. (For interpretation of the references to color in this figure legend, the reader is referred to the web version of this article.)

quartile depths were determined using R. In addition, for each species in each sampling year, the median urchin depth was identified (with 50% of urchins shallower and 50% deeper).

2.4. Temporal changes in depth

The assumptions of normality and homogeneous variances were tested using the Shapiro–Wilk normality test and the studentized Breusch–Pagan test in R. If the data met these assumptions, parametric analyses were used to determine temporal changes in depth. When the data violated these assumptions, we used the Box–Cox power transformation to transform the data. If the transformation did not improve normality or homoscedasticity of the data then non-parametric tests were used. Two-way Komolgorov–Smirnov tests were carried out for each species to compare depth distributions of trawl depths containing one or more individual among paired survey years. Linear regressions between various depth distribution parameters and survey years indicated how closely the changes in depth characteristics matched the secular changes in oceanographic variables observed over recent decades in this region (Bograd et al., 2015). The depth parameters analyzed were upper and lower limits, first and third quartiles, and mean and median depths of inhabited trawls, as well as the median depth of urchins for each species.

2.5. Temporal changes in density

Mean density for each species was calculated for each sampling date from all trawls including those where zero individuals were present. Due to the zero-inflated dataset, the implementation of data transformation had no effect on the normality nor the homogeneity of variance for any species. Thus, a Kruskal–Wallis test was used for each species to compare species density across years for the entire survey area and for each depth bin. If a significant difference was detected, a *post hoc* Dunn's test treated with a Bonferroni correction was conducted using the Pairwise Multiple Comparison of Mean Ranks Package in R.

2.6. Multivariate El Niño Southern Oscillation (ENSO) Index (MEI) relationships with depth distributions and density

Depth distribution and density data from trawl samples that contained urchins were examined for a relationship to the MEI obtained from the following NOAA website: http://www.esrl.noaa.gov/psd/enso/mei. Linear regressions for each depth parameter (see Section 2.4) and mean density (see Section 2.5) were conducted for each species' dataset with bi-monthly MEI values taken between Dec–Jan of the year before the trawl survey and Sept-Oct of the year that the SCCWRP trawl survey occurred. If the data were found to be normally distributed and have homogenous variances, then linear regression was carried out between the following metrics with bi-monthly MEI indices: various depth parameters, mean density, and depth-binned densities. Regression R^2 values indicated how closely the changes in depth characteristics and densities matched the strength of the El Niño conditions. If the t-statistic was negative, the distribution parameter was determined to shoal or density was determined to decrease during stronger El Niño conditions. In contrast, if the *t*-statistic was positive, the distribution parameter was determined to deepen or density was determined to increase during stronger El Niño conditions. If a significant regression was found with one or more bi-monthly MEI, relationships were reported with seasons rather than monthly pairs.

2.7. Dissolved oxygen and pH relationships with MEI in the SCB

To examine the relationship between ENSO cycles and DO and pH, seasonal DO data collected at 100 m, 200 m, and 300 m depth between 1994 and 2013 from 4 nearshore CalCOFI stations (line 81.8, station 46.9; line 86.7, station 35.0; line 90.0, station 30.0; line 93.3, station 30.0) were obtained from the CalCOFI website (http://calcofi.org/data.html). These stations provide a spatial overlap with the 1994–2013 trawl surveys used in this study. Estimates of pH (seawater scale) were calculated using empirical relationships with temperature and DO (Alin et al., 2012). Regression analysis of DO and pH were carried out to determine

their respective relationships with respect to time and MEI. Bi-monthly MEI indices were assigned to DO and pH values based on the date of sample collection according to the CalCOFI database. To determine the magnitudes of DO and pH changes between strong El Niño years where MEI was greater than 1 and strong La Niña years where MEI was less than -1 (strong La Niña), DO and pH in those years were compared using a t-test.

2.8. DO and pH relationships with species depth distributions and densities

Mean DO and mean pH were calculated among 4 CalCOFI stations for each survey year (4 cruises per year) and were matched with species distributions and densities depending on the approximate depth of peak density for that species (e.g., mean DO and pH at 100 m during 1994, 1998, 2003, 2008, and 2013 were matched with *L. pictus*). Collinearity between DO and pH in the study region prevented the use of multiple regression, and therefore, linear regressions of depth distributions and densities were carried out with DO and pH independently.

3. Results

3.1. Lytechinus pictus

3.1.1. Temporal changes in depth

L. pictus was found deeper in 1998 than in 2003 and 2008 (KS test: $D > 0.25$, $p < 0.05$) (Fig. 4A) (Table 1). The upper part of its range (first quartile) appeared to shoal by 1.34 m yr^{-1} from 54 m

in 1994 to 34 m in 2013 ($t_3 = -3.931$, $p = 0.03$, $R^2 = 0.78$), as did the median depth of trawls with *L. pictus* by 0.94 m yr^{-1} ($t_3 = -2.515$, $R^2 = 0.57$) from 74.5 m in 1994 to 59.5 m in 2013, but this latter relationship was not significant ($p = 0.09$). The median urchin depth shoaled by 1.44 m yr^{-1} from 86 m in 1994 and 1998 to 58 m in 2013 ($t_3 = -5.143$, $p = 0.01$, $R^2 = 0.86$). The lower depth limit appeared to shoal from 191 m in 1993 to 137 m in 2003, but was found deeper in 2013 at 189 m (Table 1).

3.1.2. Temporal changes in density

The mean density of *L. pictus* throughout the upper 200 m varied significantly among survey years (Kruskal–Wallis Test: $\chi^2 = 11.98$, $p = 0.02$) (Fig. 5A) (Table 1). *L. pictus* mean density in 2008 (0.028 indiv. m^{-2}) and 2013 (0.023 indiv. m^{-2}) was 76% and 80% lower than in 1994 (0.117 indiv. m^{-2}), respectively (post hoc Dunn's test: $p < 0.05$), while densities in 1998 (0.087 indiv. m^{-2}) and 2003 (0.038 indiv. m^{-2}) were not significantly different from any other year. When evaluated by finer 50-m depth bins, *L. pictus* density varied significantly among survey years within 51–100 m (Kruskal–Wallis Test: $\chi^2 = 12.68$, $p = 0.01$) and 101–150 m depth bins ($\chi^2 = 14.15$, $p < 0.01$) (Fig. 6A). Density within the 51–100 m depth bin declined by 74% from 0.252 indiv. m^{-2} in 1998 to 0.065 indiv. m^{-2} in 2003 (post hoc Dunn's test: $p = 0.02$). During the 2003 survey, *L. pictus* density was reduced to zero in the 151–200 m depth bin and increased in 2008, but this increase is indistinguishable from the sampling error (Fig. 6A). Survey year significantly predicted density within the 101–150 m depth bin from 1994 to 2013, with density decreasing by 0.02 indiv. m^{-2} yr^{-1} ($t_{56} = -2.956$, $p = 0.02$, $R^2 = 0.12$).
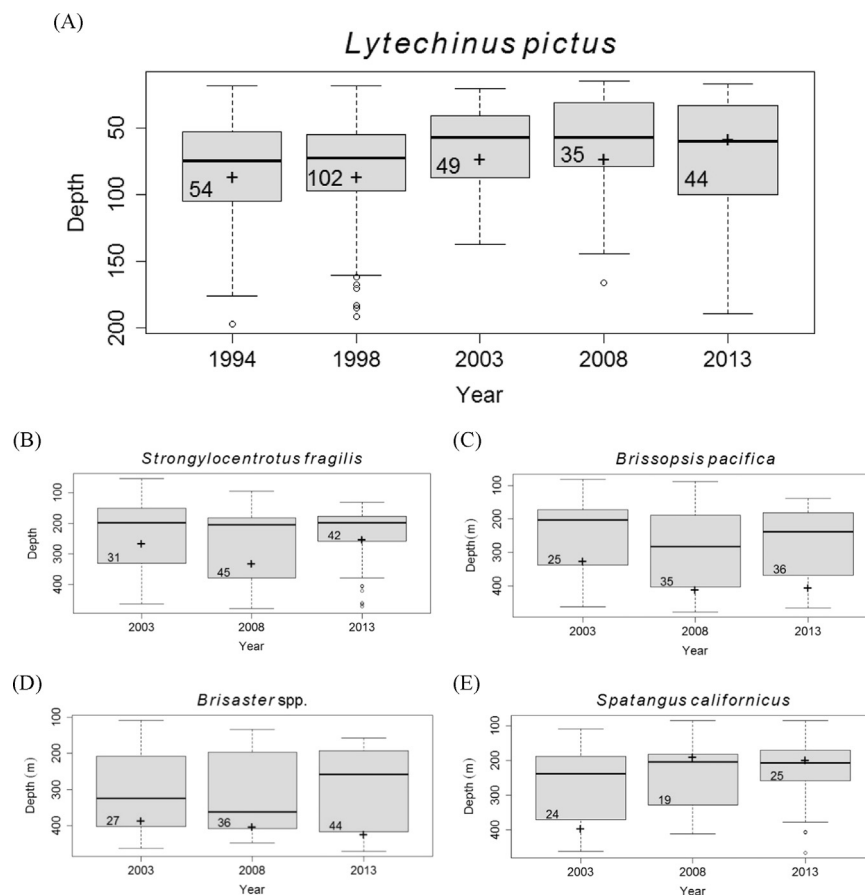
(A)

(B) (C) (D) (E)

Fig. 4. Sea urchin depth distribution boxplots for the Southern California Bight based on trawls with one or more individual of each species. Box plots represent upper and lower depth limits, first and third quartile depths, and median depth. Plus signs indicate the median depth of urchins. Numbers within each boxplot indicate number of independent trawls used for the calculation. (A) *Lytechinus pictus*. (B) *Strongylocentrotus fragilis*. (C) *Brissopsis pacifica*. (D) *Brisaster* spp. (E) *Spatangus californicus*.

Table 1
Sea urchin depth distribution metrics and density changes over time in the Southern California Bight. No Change represents a non-significant change in depth distribution metrics or density over time. Negative results indicate a consistent shallowing of depth distribution metrics or a decrease in mean density over time (p-values < 0.05 indicate a significant relationship between depth distribution metric and time or a significant difference in density among years). Positive results indicate a consistent deepening of depth distribution metrics or an increase in density over time.

Species time period	Depth range	Two-way K-S test Depth distribution	Linear regression Upper depth limit	Median trawl depth	Mean trawl depth	First quartile trawl depth	Third quartile trawl depth	Lower depth limit	Median urchin depth	Kruskal–Wallis Mean urchin density
L. pictus 1994–2013	10–200 m	Significant	Negative $p=0.03$	Negative $p=0.09$	No Change	Negative $p=0.03$	No Change	No Change	Negative $p=0.01$	Negative $p=0.02$
S. fragilis 1994–2013	10–200 m	NA		No Change	No Change	No Change	No Change	No Change	No Change	No Change
S. fragilis 2003–2013	10–500 m	Not Significant	Positive $p=0.01$	No Change	No Change	No Change	No Change	No Change	No Change	Positive $p=0.02$
B. pacifica 2003–2013	10–500 m	Not Significant	No Change	No Change	No Change	No Change	No Change	No Change	Positive $p=0.04$	No Change
Brisaster spp. 2003–2013	10–500 m	Not Significant	Positive $p=0.07$	No Change	No Change	No Change	No Change	No Change	No Change	Positive $p=0.02$
S. californicus 2003–2013	10–500 m	Not Significant	No Change	No Change	No Change	Negative $p=0.06$	Negative $p=0.10$	No Change	No Change	No Change

3.1.3. Urchin relationship with MEI

L. pictus median and first and third quartile depths were positively related to summer MEI ($F_{1,3} > 3.32$, $p < 0.05$, $R^2 > 0.70$) (Table 2), suggesting that the species occupied deeper depths during stronger El Niño conditions. In addition, the strength of El Niño conditions in the summer months significantly predicted *L. pictus* density ($t_3 = 3.978$, $p = 0.03$, $R^2 = 0.78$).

3.1.4. Depth distribution and density relationship with DO and pH

Between 1994 and 2013, *L. pictus* density in the upper 200 m was positively related to both mean DO ($t_3 = 6.121$, $p < 0.01$, $R^2 = 0.90$) and mean pH at 100 m ($t_3 = 4.535$, $p = 0.02$, $R^2 = 0.83$) (Table 3). pH significantly predicted the depths of the first quartile ($t_3 = 5.432$, $p = 0.01$, $R^2 = 0.88$), the median depth of trawls with *L. pictus* ($t_3 = 3.432$, $p = 0.04$, $R^2 = 0.73$), and the median urchin depth ($t_3 = 6.280$, $p < 0.01$, $R^2 = 0.91$) (Table 3).

3.2. Strongylocentrotus fragilis

3.2.1. Temporal changes in depth

The depth distribution of *S. fragilis* did not change in the upper 500 m from 2003 to 2013 (KS tests: $p > 0.05$) (Fig. 4B) (Table 1). The upper depth limit of *S. fragilis* was found to deepen by 7.7 m yr^{-1} on average from 53.1 m in 2003 to 130.1 m in 2013 ($t_1 = 44.46$, $p = 0.01$, $R^2 = 0.99$), but no trend was found for any other depth metric over this time period (Fig. 4B) (Table 1).

3.2.2. Temporal changes in density

The mean density of *S. fragilis* throughout the upper 200 m varied significantly among survey years from 1994–2013 (Kruskal–Wallis Test: $\chi^2 = 11.84$, $p = 0.02$) (Fig. 5B) (Table 1). There was a significant positive relationship between density in the upper 200 m and year (1994–2013), with density increasing at 0.001 indiv. m^{-2} yr^{-1} ($t_3 = 14.61$, $p = 0.03$, $R^2 = 0.77$). Post hoc Dunn's test revealed significant differences in *S. fragilis* density among years, but when treated with a Bonferroni correction, these differences became insignificant (Fig. 5B). Compared to the 2003 mean density within the upper 500 m (0.028 indiv. m^{-2}), *S. fragilis* density was 35% higher in 2008 (0.039 indiv. m^{-2}) and 133% higher in 2013 (0.067 indiv. m^{-2}) (Kruskal–Wallis Test: $\chi^2 = 7.40$, $p = 0.02$) (Fig. 5C). This resulted in an annual density increase from 2003 to 2013 by 0.003 indiv. m^{-2} yr^{-1} ($t_{440} = 1.99$, $p < 0.05$, $R^2 < 0.01$) (Table 1). At finer depth bins, *S. fragilis* density varied significantly among survey years; between 101 and 200 m, density increased from 0.038 indiv. m^{-2} in 2003 to 0.090 indiv. m^{-2} in 2008 (138% increase) and from 2008 to 0.105 indiv. m^{-2} in 2013 (17% increase) (Kruskal–Wallis Test: $\chi^2 = 6.62$, $p = 0.04$) (Fig. 5C). Although *S. fragilis* density appears to decrease in the upper 100 m between 2003 and 2013, these values correspond to very small densities ($\sim 10^{-5}$ indiv. m^{-2}), thus they are indistinguishable from sampling error.

3.2.3. Urchin relationship with MEI

S. fragilis median depths were negatively correlated with spring MEI ($t_1 = -134.5$, $p < 0.05$, $R^2 = 0.99$), and mean depths were negatively correlated with summer MEI ($t_1 = -43.2$, $p < 0.05$, $R^2 = 0.99$) (Table 2), suggesting that the species occupied shallower depths during stronger El Niño conditions. In addition, the strength of El Niño conditions in the summer months was negatively related to *S. fragilis* density ($R^2 = 0.98$), but this relationship was not significant ($p = 0.06$).

3.2.4. Depth distribution and density relationship with DO and pH

Between 2003 and 2013, *S. fragilis* density in the upper 500 m was significantly predicted by mean DO at 200 m ($t_1 = -13.9$, $p < 0.05$, $R^2 = 0.99$), but not pH at 200 m. However, *S. fragilis* density in the upper 200 m between 1994 and 2013 was
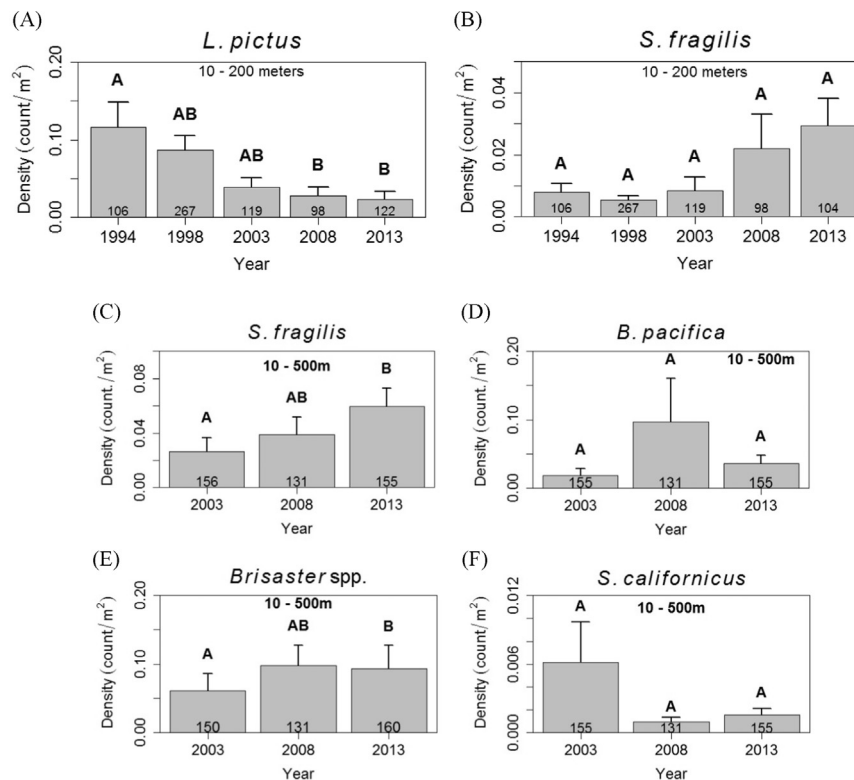
Fig. 5. Mean density (+1 SE) of sea urchins throughout the entire Southern California Bight survey region. For *Lytechinus pictus*, surveys dating back to 1994 covered depths from 10 to 200 m. For deeper species, surveys were extended to 500 m in 2003. Letter indicates significant difference resulting from a Kruskal–Wallis and *post hoc* Dunn's tests. Numbers within each barplot indicate the number of independent trawls used for the calculation. (A) *Lytechinus pictus*. (B) *Strongylocentrotus fragilis* (upper 200 m from 1994 to 2013). (C) *Strongylocentrotus fragilis* (upper 500 m from 2003 to 2013). (D) *Brissopsis pacifica*. (E) *Brisaster* spp. (F) *Spatangus californicus*.
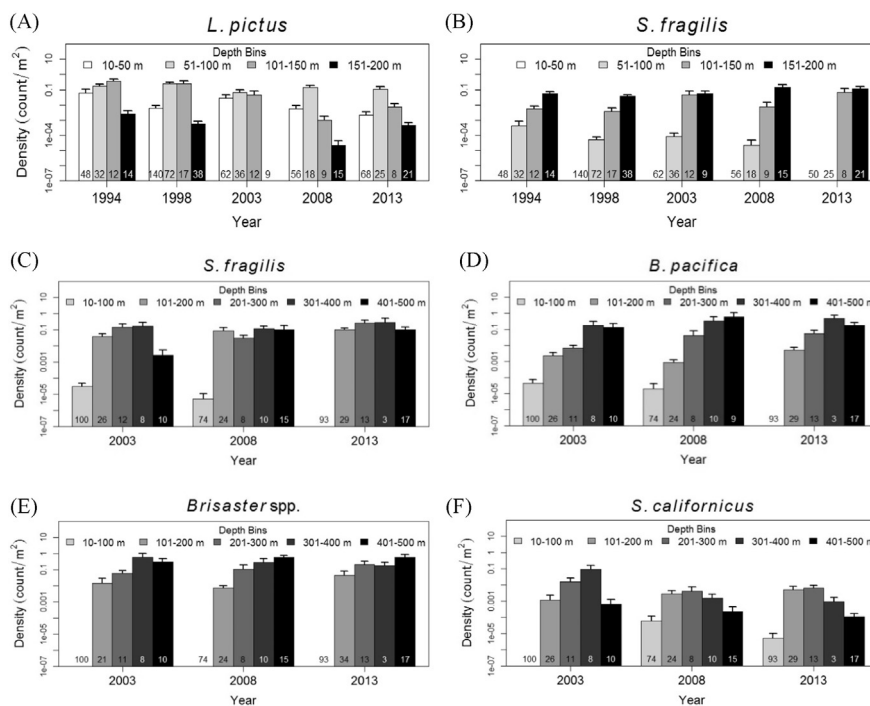

Fig. 6. Mean log-scale density (+1 SE) of (A) *Lytechinus pictus*. (B) and (C) *Strongylocentrotus fragilis*. (D) *Brissopsis pacifica*. (E) *Brisaster* spp. (F) *Spatangus californicus* in the Southern California Bight from 1994 to 2013. Urchins were separated into 50-m depth bins (*L. pictus and S. fragilis*) and 100-m depth bins (other species). Numbers within each barplot indicate number of independent trawls used for calculation.

Table 2
Linear regression results showing relationships of sea urchin depth distribution metrics to ENSO conditions based on bi-monthly MEI values. Negative relationships indicate shoaling of depth distribution metrics and decreasing density in response to stronger El Niño-like conditions (e.g., higher oxygen, higher pH). Positive relationships indicate deepening of depth distribution metrics and increasing density in response to stronger El Nino-like conditions (e.g., higher oxygen, higher pH). p-Values < 0.05 indicate a significant relationship between depth distribution metrics and density with MEI values. NS indicates a non-significant relationship, and NA results indicate Not Available because these analyses were not ecologically relevant.

Response to increasing strength of El Niño conditions	Upper depth limit	First quantile depth	Median trawl depth	Third quantile depth	Mean trawl depth	Lower limit depth	Mean urchin density	Median urchin depth
L. pictus	NS	Positive $p < 0.05$	Positive $p < 0.05$	Positive $p < 0.05$	NS	NS	Positive $p < 0.05$	Positive $p = 0.07$
S. fragilis 10–200 m	NA						NS	NA
S. fragilis 10–500 m	Negative $p = 0.09$	Negative $p = 0.06$	Negative $p < 0.05$	NS	Negative $p < 0.05$	Negative $p < 0.05$	Negative $p = 0.06$	Negative $p = 0.07$
B. pacifica	Negative $p < 0.05$	Negative $p = 0.07$	Negative $p < 0.05$	Negative $p < 0.01$	Negative $p < 0.01$	Negative $p < 0.05$	Negative $p < 0.05$	Negative $p = 0.12$
Brisaster spp.	Positive $p < 0.05$	NS	Positive $p = 0.06$	Positive $p < 0.01$	NS	Positive $p < 0.01$	Negative $p = 0.10$	Negative $p = 0.07$
S. californicus	NS	NS	NS	NS	NS	Positive $p < 0.05$	NS	NS

Table 3
Linear regression results of sea urchin depth distribution metrics and density with mean dissolved oxygen (DO) and pH in the Southern California Bight. Significant relationships with DO or pH at 100 m, 200 m, or 300 m are listed as response variable ($+$ or $−$ sign of relationships). Negative relationships ($−$) indicate deepening of depth distribution metrics and increasing density in response to decreasing DO or decreasing pH ($p < 0.05$). Positive relationships ($+$) indicate shallowing of depth distribution metrics and decreasing density in response to decreasing DO or decreasing pH ($p < 0.05$). NS indicates a non-significant relationship, and NA results indicate Not Available because these analyses were not ecologically relevant.

Species	Years analyzed	100 m DO	100 m pH	200 m DO	200 m pH	300 m DO	300 m pH
L. pictus 10–200 m	1994–2013	Density ($+$)	Density; 1st Quartile Depth; Median Trawl Depth; Median Urchin Depth ($+$)	Density; 1st Quartile Depth; Median Trawl Depth; Median Urchin Depth ($+$)		NA	NA
S. fragilis 10–200 m	1994–2013	NS	Density ($−$)	NS	NS	NA	NA
S. fragilis 10–500 m	2003–2013	NS	NS	Density ($−$)	NS	NS	NS
B. pacifica 10–500 m	2003–2013	NS	NS	NS	NS	NS	NS
Brisaster spp. 10–500 m	2003–2013	Upper Depth Limit ($−$)	Upper Depth Limit; Median Urchin Depth (-)	NS	Upper Depth Limit; Median Urchin Depth ($−$)	NS	NS
S. californicus 10–500 m	2003–2013	1st Quartile Depth ($+$)	1st Quartile Depth; 3rd Quartile Depth ($+$)	3rd Quartile Depth ($+$)	1st Quartile Depth; 3rd Quartile Depth ($+$)	NS	NS

significantly predicted by pH at 100 m ($t_3 = -3.24$ $p < 0.05$, $R^2 = 0.99$) (Table 3).

3.3. Burrowing urchins

3.3.1. Temporal changes in depth

The depth distributions of each burrowing urchin species (*Brissopsis pacifica*, *Brisaster* spp. and *Spatangus californicus*) did not vary significantly in the upper 500 m from 2003 to 2013 (KS tests: $p > 0.05$) (Fig. 4C–E) (Table 1). The first and third quartile depths of *B. pacifica* appeared to shoal, but these relationships were not significant (Fig. 4C). The median depth of *Brisaster* spp. deepened by 3.85 m yr^{-1} ($t_1 = 14.82$, $p = 0.04$, $R^2 = 0.99$) (Fig. 4D). From 2003 to 2013, the upper limit, first and third quartiles, mean and median depths of *S. californicus* appeared to shoal by 2–11 m yr^{-1} (Fig. 4E) but again, these relationships were not significant.

3.3.2. Temporal changes in density

Neither *B. pacifica* nor *S. californicus* density within the upper 500 m significantly varied across years (Kruskal–Wallis Test: *B. pacifica*: $\chi^2 = 4.85$, $p = 0.08$; *S. californicus*: $\chi^2 = 0.13$, $p = 0.94$) (Fig. 5D, F). *Brisaster* spp. density did vary significantly within the upper 500 m from 2003 to 2013 (Kruskal–Wallis Test: $\chi^2 = 7.66$, $p = 0.02$), but density did not show a consistent change with time

($p = 0.24$) (Fig. 5E) (Table 1). Compared to 2003 mean *Brisaster* spp. density (0.06 indiv. m^{-2}), density was 61% higher in 2008 and 54% higher in 2013 (post hoc Dunn's test: $p < 0.05$).

B. pacifica and *S. californicus* density within each 100-m depth bin did not significantly vary among survey years (Fig. 6D, F). The mean *B. pacifica* density increased at a rate of 0.03 indiv. m^{-2} yr^{-1} within the 301–400 m depth bin from 2003 to 2013 ($t_1 = 166.6$, $p < 0.01$, $R^2 > 0.99$) and at a rate of 0.005 indiv. m^{-2} yr^{-1} within the 201–300 m depth bin from 2003 to 2013, although this latter relationship was not significant ($p = 0.13$) (Fig. 6D). From 2003 to 2013, the mean density of *S. californicus* increased within the 101–200 m depth bin and decreased within the 201–300 m, 301–400 m, and 401–500 m depth bins, but these relationships were not significant ($p > 0.05$) (Fig. 6F). *Brisaster* spp. density varied significantly among survey years within the 101–200 m depth bin (Kruskal–Wallis Test: $\chi^2 = 8.14$, $p = 0.02$), but mean density did not change consistently with time ($p = 0.36$) (Fig. 6E).

3.3.3. Depth and density relationship with MEI

B. pacifica mean, median, third quartile, and lower limit depths were negatively related to fall and winter MEI ($t_1 < -10$, $p < 0.05$, $R^2 = 0.99$), and upper limit depth was negatively related to summer MEI ($t_1 < -14$, $p < 0.05$, $R^2 = 0.99$) (Table 2), suggesting that the species occupied shallower depths during stronger El Niño

conditions. In addition, the strength of El Niño conditions in the spring and summer months predicted *B. pacifica* density ($F_{1,1} < -16$, $p < 0.05$, $R^2 = 0.99$). *Brisaster* spp. upper and lower limit

(A)

Oxygen at 4 nearshore CalCOFI stations
1994 - 2013

(B)

pH at 4 nearshore CalCOFI stations
1994 - 2013

Fig. 7. Changes in (A) dissolved oxygen (DO) concentration and (B) pH for CalCOFI stations (line 81.8, station 46.9; line 86.7, station 35.0; line 90.0, station 30.0; line 93.3, station 30.0) at 100 m (gray), 200 m (blue), and 300 m (black) between 1994 and 2013 in the Southern California Bight. Depth-specific regression lines for DO and pH were all significantly related to time. (For interpretation of the references to color in this figure legend, the reader is referred to the web version of this article.)

depths were positively related to summer MEI ($F_{1,1} > 23$, $p < 0.05$, $R^2 = 0.99$) (Table 2), suggesting that this species occupied deeper depths (or was more likely to be on the surface in deeper waters) during stronger El Niño conditions. *Brisaster* spp. third quartile depth was positively related to spring MEI ($t_1 = 10.4$, $p < 0.05$, $R^2 = 0.99$), and while spring MEI was also positively related to *Brisaster* spp. density, this latter relationship was not significant ($p = 0.10$) (Table 2). *S. californicus* lower depth limit was positively related to spring MEI ($t_1 = 13.4$, $p < 0.05$, $R^2 = 0.99$), but no other depth distribution metric or density were related to any bi-monthly MEI (Table 2).
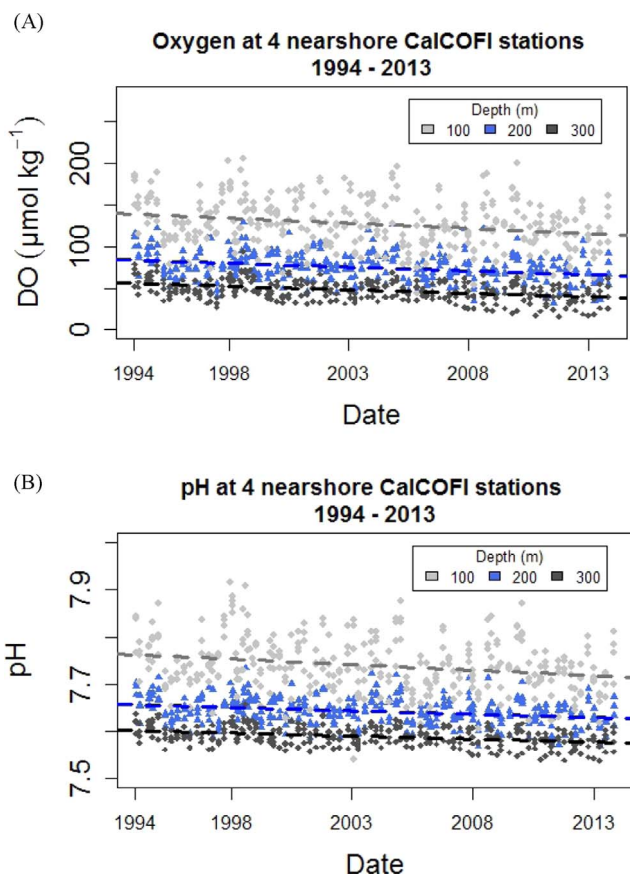
3.3.4. Depth distribution and density relationship with DO and pH

The upper depth limit of *Brisaster* spp. was negatively related to mean DO at 100 m ($t_1 = -15.35$, $p = 0.04$, $R^2 = 0.99$), pH at 100 m ($t_1 = -32.56$, $p = 0.02$, $R^2 = 0.99$), and pH at 200 m ($t_1 = -54.13$, $p = 0.01$, $R^2 = 0.99$). The median depth of *Brisaster* spp. was also negatively related to pH at 100 m ($t_1 = -34.34$, $p = 0.02$, $R^2 = 0.99$), and pH at 200 m ($t_1 = -12.75$, $p < 0.05$, $R^2 = 0.99$). The 75% quartile of *S. californicus* was positively related to both DO and pH at 100 m and 200 m, while the 25% quartile was only positively related to pH (Table 3). No significant relationships between *B. pacifica* depth metrics or density and mean DO or pH were found (Table 3).

3.4. Dissolved oxygen and pH relationships with time and MEI in the SCB

Between 1994 and 2013, DO was negatively related to survey year at 100 m ($t_{329} = -4.551$, $p < 0.001$, $R^2 = 0.06$), 200 m ($t_{329} = -5.551$, $p < 0.001$, $R^2 = 0.08$), and 300 m ($t_{328} = -7.982$, $p < 0.001$, $R^2 = 0.16$) (Fig. 7A), as was pH at 100 m ($t_{329} = -4.6$, $p < 0.001$, $R^2 = 0.05$), 200 m ($t_{329} = -5.434$, $p < 0.001$, $R^2 = 0.08$), and 300 m ($t_{328} = -7.347$, $p < 0.001$, $R^2 = 0.14$) (Fig. 7B). DO and pH values at 100 m were positively related to MEI values from 1994 to 2013 (DO: $t_{336} = 4.306$, $p < 0.001$, $R^2 = 0.05$; pH: $t_{336} = 5.26$, $p < 0.001$, $R^2 = 0.07$), with DO increasing at a rate of 3.166 µmol DO kg^{-1} MEI unit^{-1} (Fig. 8A), and pH increasing at a rate of 0.015 pH units MEI unit^{-1} (Fig. 8C). At 100 m in the SCB, mean DO during strong El Niño years (MEI > 1) between 1994 and 2013 (145.5 ± 29.8 µmol kg^{-1} [mean ± 1 SD]) was found to be 25%

(A) **Oxygen at 100 m vs. MEI**
by CalCOFI station (1994 - 2013)

(B) **1994-2013**

(C) **pH at 100 m vs. MEI**
by CalCOFI station (1994 - 2013)
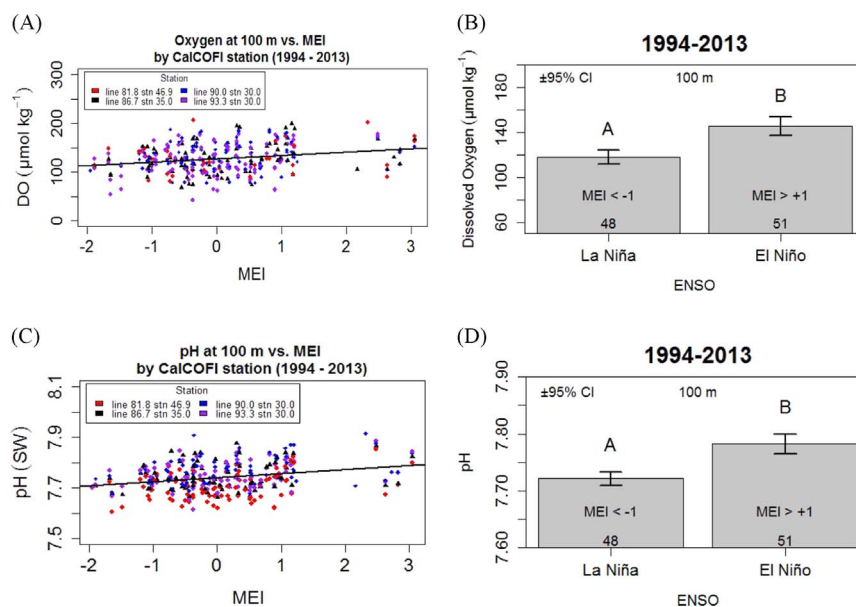
(D) **1994-2013**

Fig. 8. (A) Dissolved oxygen (DO) concentration and (C) pH as a function of MEI (1994–2013) for CalCOFI stations (line 81.8, station 46.9; line 86.7, station 35.0; line 90.0, station 30.0; line 93.3, station 30.0) at 100 m in the Southern California Bight. (B) Mean DO concentration and (D) mean pH ± 95% confidence intervals for MEI < −1.0 (La Niña conditions) and MEI > 1.0 (El Niño conditions).

higher than during strong La Niña years (118.0 ± 22.3 μmol kg^{-1}; t-Test: $t_{94} = -5.19$, $p < 0.001$) (Fig. 8B), while mean pH during strong El Niño years (7.78 ± 0.06) was a significant 0.06 pH units higher than during strong La Niña years (7.72 ± 0.04; t-Test: $t_{87} = -5.78$, $p < 0.001$; Fig. 8D).

4. Discussion

Observed temporal trends in echinoid species depth distributions and densities (Table 1, Figs. 4–6) suggest that deep-dwelling urchin species may have experienced habitat expansion upslope in the upper 500 m and shallower-dwelling urchin species may have experienced habitat compression in the upper 200 m over the past 21 years due to multiple climate stressors in the SCB such as DO, temperature, pH, Ω, and pCO$_2$ (Alin et al. 2012; Frieder et al., 2012; Nam et al. 2015). Trawl survey data reflect (1) shoaling of depth distributions and possible habitat compression in *L. pictus*, and (2) habitat expansion or upslope shifts in *Brisaster* spp. and *S. californicus* (Table 1). Examination of DO and pH data in the upper 200 m at single nearshore CalCOFI stations within the study region between 1994 and 2013 indicates that a change in habitation depth of 20–30 m can yield a 15–63 μmol kg^{-1} change in DO exposure and a 0.03–0.15 unit change in pH exposure (Appendix 1). Although our data did not allow us to assess the potential intensification of the OMZ at depths greater than 500 m, these deep species may have responded to secular deoxygenation and acidification in the SCB, but may have also been influenced by variability in environmental conditions such as oxygen and pH associated with ENSO (Fig. 8). ENSO-related variations in the system can affect major population drivers such as food availability, food quality, and competition. However, other secular changes in the SCB over this time period such as increasing primary productivity and frontal frequency (Bograd et al., 2015; Kahru et al., 2012), intensifying upwelling winds (Sydeman et al., 2014), and warming in the upper 200 m (Di Lorenzo et al., 2005) are potential covariates that could contribute to interannual variability in suitability of urchin habitat. In addition, the positive and negative relationships of population size and distributions with MEI (Table 2), indicate that other factors may have driven temporal change in population densities and distributions in this system.

While changes in benthic fish and invertebrate populations in response to climate events are expected, our results indicate that these effects are species-specific (Arntz et al., 2006). A significant positive relationship between MEI and *L. pictus* density suggest stronger El Niño conditions favor this species, while negative relationships of *S. fragilis* and *B. pacifica* density with MEI suggest they are negatively affected by El Niño conditions. Significant relationships of *L. pictus* and *S. fragilis* density with annual means of DO and pH suggest that these species are affected by these environmental factors (Table 3), and opposite density trends suggest competition in the upper 200 m may also limit *L. pictus* and favor *S. fragilis* (Fig. 5A, B). Interpreting these differences requires a deeper understanding of life history, food sources, and spatio-temporal dynamics.

The urchin species discussed are grossly understudied despite the potentially high impact they may have on the deep-sea community, and specific mechanisms of population structure change cannot be revealed with the current sampling design. Possible lags in species response (i.e. changes in depth distribution or density) to environmental variables likely exist depending on the species' life history (Glover et al., 2010). For example, although the lifespan of *L. pictus* is unknown, the estimated lifespan of the congener, *L. variegatus*, is < 5 yr (Watts et al., 2007; Bodnar and Coffman, 2016). Five years after the strong El Niño of 1998, the mean density of *L. pictus* declined by 56%; this decline persisted until 2013 (Fig. 5A).

Thus, it is possible that *L. pictus* populations responded to kelp food availability at shorter time scales than the longer-lived *S. fragilis* (Taylor et al., 2014), and trawl surveys at 5-yr intervals could not reveal the influence of ENSO events on *L. pictus* populations.

To determine the feasibility of urchin migration as a possible mechanism for the observed depth changes, we estimated the average slope of the continental shelf and slope in the SCB using Google Earth. We found that a 10 m reduction in depth for the shallower, *L. pictus* on the shelf might occur over a 1 km horizontal distance. Although the average travel speed of adult *L. pictus* is unknown, Pisut (2004) found the average speed of *L. variegatus* to be ~0.7 m h^{-1}, and Barry et al. (2014) found the average speed of *S. fragilis* to be ~0.25 m h^{-1}. Therefore, it is feasible for individuals to migrate 1 km in 5 years, so depth changes may reflect migration rather than mortality and recruitment. The significant decrease in density of *L. pictus* in the SCB over the time period of this study however, would suggest that mortality and lowered recruitment did occur. Potential mechanisms for increased mortality and lower recruitment for *L. pictus* over time include physiological intolerance to low pH or low DO, increased predation, increased competition and/or reduced larval supply.

L. pictus and *S. fragilis* are epibenthic omnivores that primarily feed on allochthonous kelp detritus (Barry et al., 2014; Thompson et al., 1983; Fig. 2A, B) that originates from the inshore zone of the coastal SCB (Dayton, 1985; Krumhansl and Scheibling, 2012; Parnell et al., 2010). During and following El Niño years, anomalously higher nearshore sea surface temperatures off the southern California coast can persist for at least 2 years (McGowan et al., 1998). Results of warmer surface waters include intensified stratification, reduced upwelling, and reduced primary production by phytoplankton (Barber and Chavez, 1983; Contreras et al., 2007) and kelp (Tegner and Dayton, 1987). This could negatively affect the availability of autochthonous food in the form of sinking organic matter (phytodetritus) for deep-sea benthic communities including epibenthic and burrowing urchins (Lange et al., 2000 Gutierrez et al., 2000; Levin et al., 2002; Sellanes and Neira, 2006), and may also explain the negative relationships between MEI and *S. fragilis* and *B. pacifica* densities (Table 2). Alternatively, burrowing spatangoid urchins may benefit from increased input of terrestrial organic matter during stronger El Niño years as a result of increased runoff from winter storms (Lange et al., 2000, and others). However, sinking organic matter of terrestrial origin has been found to have lower protein content, higher C: N ratios and lower nutritional quality than marine sources (Cowie et al., 2009). Stable isotope analysis of deposit-feeding urchins combined with gonad analyses may help to better understand the differential effects of food source quality and origin on reproduction and fitness during El Niño and non-El Niño years.

Winter storms during El Niño years can also dislodge and export significant kelp forest biomass (Dayton and Tegner, 1984; Parnell et al., 2010), which may temporarily increase supply of allochthonous food to deep-sea habitats in the form of kelp detritus (Harrold et al., 1998; Vetter and Dayton, 1998). However, low overall production of *Macrocystis pyrifera* kelp canopy during summer El Niño years should limit food and reduce urchin populations (Edwards 2004 and references therein). While this understanding could explain the negative relationship between MEI and *S. fragilis*, it cannot explain the opposite response of *L. pictus* at depths less than 200 m. Instead the higher DO and pH associated with El Niño conditions may favor *L. pictus* (Fig. 8). However, the lower depth bins of *L. pictus* (101–200 m) overlap with *S. fragilis*, so it is possible that during strong El Niño years when there is limited food, a competitive interaction between the two urchins occurs. Density data support the hypothesis that these two species interact in the upper 200 m (Fig. 5A, B), and possibly within smaller depth bins where they coexist (Fig. 6A, B), but

further analysis is required to test this. It is also possible that decadal oscillations in climate may affect trends in density. For example, changes in the NPGO and PDO in the last decade can affect bottom-up processes that likely influence entire marine communities (Bell et al., 2015; Di Lorenzo et al., 2008; Miller et al., 2015). A better understanding of how food source dynamics interact with stressors to influence margin urchin populations is required, particularly regarding the origin and fate of autochthonous and allochthonous food sources in response to physical oceanographic processes affected by ENSO cycles.

In addition to food availability, climate-related perturbations in the physical, chemical and biological structure of the environment can result in shifts in the vertical zonation of entire land- and seascapes (Cheung et al., 2011; Parmesan, 2006; Wishner et al., 2013). For example, La Niña years often follow El Niño years (Table 1) and are characterized by enhanced upwelling and prolonged exposure to hypoxic and acidic conditions (Booth et al., 2014; Nam et al., 2011). This pattern of low food years (El Niño), followed by low-oxygen, low-pH periods (La Niña) can represent a one-two punch and be detrimental to population growth (Ramajo et al., 2016). As OMZs expand and OLZs shoal, waters low in pH and high in CO_2 are also expected to creep upslope (Gruber et al., 2012) and onto the shelf (Feely et al., 2008). This may exacerbate negative consequences for vulnerable larval stages of calcifying urchin species adapted to shallower conditions by increasing metabolic energy demand (Pan et al., 2015), but it is unclear if larvae of deep-sea species have greater tolerance to future climate change than those of shallower species (Jager et al., 2016; Stumpp et al., 2012). These secular trends of deoxygenation and ocean acidification may induce a competitive advantage for deeper urchins (e.g. *S. fragilis*, *B. pacifica* and *Brisaster* spp.) equipped with the adaptive machinery to persist in hypoxic and hypercapnic environments over those restricted by such conditions (Byrne and Przeslawski, 2013; Portner et al., 2005; Taylor et al., 2014). Deep-sea, *in situ* manipulation experiments simulated future deep-ocean acidification and revealed longer foraging time and no difference in speed of adult *S. fragilis* under acidic conditions, which implied tolerance to acidification (Barry et al., 2014). Behavioral responses coupled with adaptive capacities for *S. fragilis* to regulate acid-base balance under acidic conditions (Taylor et al., 2014) and low oxygen-consumption rates under hypoxic conditions (Thompson et al., 1983) may induce a competitive advantage over *L. pictus*, which could explain the increase in *S. fragilis* density by 174% in the 101–200 m depth bin zone from 2003 to 2013 (Fig. 6A, B). Higher oxygen or pH limits in *L. pictus* may also explain the 56% decrease from 10 to 200 m from 2003 to 2013 given the positive relationship with oxygen and pH (Fig. 7A, B; Table 3).

Despite statistically insignificant density differences among years, *B. pacifica* and *Brisaster* spp. may be better competitors than *S. californicus* echinoids in a deoxygenated, acidic future. A shoaling of median depth of 50% and a density decrease of 75% from 2003 to 2013 suggests habitat compression in *S. californicus* (Figs. 4F, 5F). As infaunal burrowers, heart urchins are exposed to even more reduced conditions than that of overlying OMZ and OLZ waters (Reimers et al., 1990). Despite the function of fascioles, which direct currents over respiratory tube feet, burrowing urchins are still exposed to surrounding pore water that is reduced in pH and oxygen relative to near-bottom waters; this has been found in both *in situ* observations of sediment pore-water chemistry (Reimers et al., 1990) and laboratory experiments focused on burrowing urchins (Vopel et al., 2007). Accordingly, their distributions and peak densities indicate that they are tolerant of extremely low-oxygen, high-CO_2 environments (Moffitt et al., 2015).

Burrowing urchins in the eastern Pacific OMZ occur in dense patches (Thompson et al., 1993; Thompson and Jones, 1987) and contribute to significant nutrient recycling processes through bioturbation of sediments (Lohrer et al., 2004; Lohrer et al., 2005). Our density estimates likely underestimated the subsurface density of spatangoid heart urchins in the SCB since otter trawls cannot accurately sample all the urchins, which may dwell as deep as 20 cm and are best sampled by boxcorers (Kanazawa, 1992; Thompson and Jones, 1987). As such, trends of shoaling depth distributions and increasing density of *Brisaster* spp. associated with deoxygenation could simply reflect movement of heart urchins to the surface to access more oxygenated waters (i.e. higher catchability). It is interesting to note the varying responses to El Niño among the three burrowing spatangoid urchin species in the upper 500 m (Table 2). Further evidence for oxygen limitation in *Brisaster* spp. and *S. californicus* may be inferred from their deepening distributions during stronger El Niño years (Table 2). While density decreases during stronger El Niño years may be explained by the overall decrease in food availability in the SCB (Nichols et al., 1989), it is likely that competitive interactions occur among *B. pacifica*, *Brisaster* spp. and *S. californicus* during years when food is limited (Dayton and Hessler, 1972).

Future studies focusing on adaptations to combined hypoxia, hypercapnia, and food limitation in different deep-sea urchin species are needed. Phenomena such as the presence and activity of sulfide-oxidizing gut microbes (Thorsen, 1998) and resource partitioning (Thompson et al., 1983) among competitors could provide further insight into how deep-margin echinoids respond to future climate change.

Appendix A. Supplementary material

Supplementary data associated with this article can be found in the online version at http://dx.doi.org/10.1016/j.dsr2.2016.08.012.

References

Alin, S.R., Feely, R.A., Dickson, A.G., Hernandez-Ayon, J.M., Juranek, L.W., Ohman, M.D., Goericke, R., 2012. Robust empirical relationships for estimating the carbonate system in the southern California Current System and application to CalCOFI hydrographic cruise data (2005–2011). J. Geophys. Res. 117.

Arntz, W.E., Gallardo, V.A., Gutiérrez, D., Isla, E., Levin, L.A., Mendo, J., Neira, C., Rowe, G.T., Tarazona, J., Wolff, M., 2006. El Niño and similar perturbation effects on the benthos of the Humboldt, California, and Benguela Current upwelling ecosystems. Adv. Geosci. 6, 243–265.

Barber, R.T., Chavez, F.P., 1983. Biological consequences of El Niño. Science 222, 1203–1210.

Barry, J.P., Lovera, C., Buck, K.R., Peltzer, E.T., Taylor, J.R., Walz, P., Whaling, P.J., Brewer, P.G., 2014. Use of a free ocean CO_2 enrichment (FOCE) system to

evaluate the effects of ocean acidification on the foraging behavior of a deep-sea urchin. Environ. Sci. Technol. 48, 9890–9897.

Bell, T.W., Cavanaugh, K.C., Reed, D.C., Siegel, D.A., 2015. Geographical variability in the controls of giant kelp biomass dynamics. J. Biogeogr. 42, 2010–2021.

Bjerknes, J., 1966. A possible response of atmospheric Hadley circulation to equatorial anomalies of ocean temperature. Tellus 18, 820–829.

Bodnar, A.G., Coffman, J.A., 2016. Maintenance of somatic tissue regeneration with age in short- and long-lived species of sea urchins. Aging Cell. http://dx.doi.org/10.1111/acel.12487.

Bograd, S.J., Buil, M.P., Di Lorenzo, E., Castro, C.G., Schroeder, I.D., Goericke, R., Anderson, C.R., Benitez-Nelson, C., Whitney, F.A., 2015. Changes in source waters to the Southern California Bight. Deep-Sea Res. 112 (Pt. II), 42–52.

Bograd, S.J., Castro, C.G., Di Lorenzo, E., Palacios, D.M., Bailey, H., Gilly, W., Chavez, F.P., 2008. Oxygen declines and the shoaling of the hypoxic boundary in the California Current. Geophys. Res. Lett. 35.

Booth, J.A.T., McPhee-Shaw, E.E., Chua, P., Kingsley, E., Denny, M., Phillips, R., Bograd, S.J., Zeidberg, L.D., Gilly, W.F., 2012. Natural intrusions of hypoxic, low pH water into nearshore marine environments on the California coast. Cont. Shelf Res. 45, 108–115.

Booth, J.A.T., Woodson, C.B., Sutula, M., Micheli, F., Weisberg, S.B., Bograd, S.J., Steele, A., Schoen, J., Crowder, L.B., 2014. Patterns and potential drivers of declining oxygen content along the southern California coast. Limnol. Oceanogr. 59, 1127–1138.

Byrne, M., Przeslawski, R., 2013. Multistressor impacts of warming and acidification of the ocean on marine invertebrates' life histories. Integr. Comp. Biol. 53, 582–596.

Cheung, W.W.L., Meeuwig, J.J., Lam, V.W.Y., 2011. Ecosystem-based fisheries management in the face of climate change. In: Christensen, V., Maclean, J. (Eds.), Ecosystem Approaches to Fisheries. A Global Perspective Cambridge University Press, New York, pp. 171–188.

Contreras, S., Pantoja, S., Neira, C., Lange, C.B., 2007. Biogeochemistry of surface sediments off Concepción (~36°S), 75. El Niño vs. non-El Niño conditions. Progr. Oceanogr, Chile, pp. 576–585.

Cowie, G.L., Mowbray, S., Lewis, M., Matheson, H., McKenzie, R., 2009. Carbon and nitrogen elemental and stable isotopic compositions of surficial sediments from the Pakistan margin of the Arabian Sea. Deep-Sea Res. II (56), 271–282.

Dayton, P.K., 1985. The structure and regulation of some South American kelp communities. Ecol. Monogr., 447–468.

Dayton, P.K., Hessler, R.R., 1972. Role of biological disturbance in maintaining diversity in the Deep Sea. Deep-Sea Res 19, 199–208.

Dayton, P.K., Tegner, M.J., 1984. Catastrophic storms, El Niño, and patch stability in a southern California kelp community. Science 224, 283–285.

Di Lorenzo, E., Miller, A.J., Schneider, N., McWilliams, J.C., 2005. The warming of the California current system: dynamics and ecosystem implications. J. Phys. Oceanogr. 35, 336–362.

Di Lorenzo, E., Schneider, N., Cobb, K.M., Franks, P.J.S., Chhak, K., Miller, A.J., McWilliams, J.C., Bograd, S.J., Arango, H., Curchitser, E., Powell, T.M., Riviere, P., 2008. North Pacific Gyre Oscillation links ocean climate and ecosystem change. Geophys. Res. Lett. 35.

Dupont, S., Ortega-Martinez, O., Thorndyke, M., 2010. Impact of near-future ocean acidification on echinoderms. Ecotoxicology 19, 449–462.

Edwards, M.S., 2004. Estimating scale-dependency in disturbance impacts: El Niños and giant kelp forests in the northeast Pacific. Oecologia 138, 436–447.

Feely, R.A., Sabine, C.L., Hernandez-Ayon, J.M., Ianson, D., Hales, B., 2008. Evidence for upwelling of corrosive "acidified" water onto the continental shelf. Science 320, 1490–1492.

Frieder, C.A., 2014. Present-day nearshore pH differentially depresses fertilization in congeneric sea urchins. Biol. Bull. 226, 1–7.

Frieder, C.A., Nam, S.H., Martz, T.R., Levin, L.A., 2012. High temporal and spatial variability of dissolved oxygen and pH in a nearshore California kelp forest. Biogeosciences 9, 3917–3930.

Gilly, W.F., Beman, J.M., Litvin, S.Y., Robison, B.H., 2013. Oceanographic and biological effects of shoaling of the oxygen minimum zone. Annu. Rev. Mar. Sci. 5, 393–420.

Glover, A.G., Gooday, A.J., Bailey, D.M., Billett, D.S.M., Chevaldonné, P., Colaco, A., Copley, J., Cuvelier, D., Desbruyeres, D., Kalogeropoulou, V., Klages, M., 2010. Temporal change in deep-sea benthic ecosystems: a review of the evidence from recent time-series studies. Adv. Mar. Biol. 58, 1–95.

Gruber, N., 2011. Warming up, turning sour, losing breath: ocean biogeochemistry under global change. Philos. Trans. R. Soc. A 369, 1980–1996.

Gruber, N., Hauri, C., Lachkar, Z., Loher, D., Frolicher, T.L., Plattner, G.K., 2012. Rapid progression of ocean acidification in the California current system. Science 337, 220–223.

Gutierréz, D., Gallardo, V.A., Mayor, S., Neira, C., Vásquez, C., Sellanes, J., Rivas, M., Soto, A., Carrasco, F., Baltazar, M., 2000. Effects of dissolved oxygen and fresh organic matter on the bioturbation potential of macrofauna in sublittoral sediments off Central Chile during the 1997/1998 El Niño. Mar. Ecol. Prog. Ser 202, 81–99.

Harrold, C., Light, K., Lisin, S., 1998. Organic enrichment of submarine-canyon and continental-shelf benthic communities by macroalgal drift imported from nearshore kelp forests. Limnol. Oceanogr. 43, 669–678.

Helly, J.J., Levin, L.A., 2004. Global distribution of naturally occurring marine hypoxia on continental margins. Deep-Sea Res. II 51, 1159–1168.

Hofmann, G.E., Barry, J.P., Edmunds, P.J., Gates, R.D., Hutchins, D.A., Klinger, T., Sewell, M.A., 2010. The effect of ocean acidification on calcifying organisms in marine ecosystems: an organism-to-ecosystem perspective. Annu. Rev. Ecol. Evol. S 41, 127–147.

Hood, S., Mooi, R., 1998. Taxonomy and phylogenetics of extant Brisaster (Echinoidea: Spatangoida). In: Balkema, A.A. (Ed.), Echinoderms. International Publishers, San Francisco, pp. 681–686.

Ito, T., Deutsch, C., 2013. Variability of the oxygen minimum zone in the tropical North Pacific during the late twentieth century. Glob. Biogeochem. Cy 27, 1119–1128.

Jager, T., Ravagnan, E., Dupont, S., 2016. Near-future ocean acidification impacts maintenance costs in sea-urchin larvae: Identification of stress factors and tipping points using a DEB modelling approach. J. Exp. Mar. Biol. Ecol. 474, 11–17.

Kahru, M., Kudela, R.M., Manzano-Sarabia, M., Mitchell, B.G., 2012. Trends in the surface chlorophyll of the California Current: merging data from multiple ocean color satellites. Deep-Sea Res 77–80 (Pt. II), 89–98.

Kanazawa, K.I., 1992. Adaptation of test shape for burrowing and locomotion in spatangoid echinoids. Palaeontology 35, 733–750.

Keller, A.A., Wallace, J.R., Horness, B.H., Hamel, O.S., Stewart, I.J., 2012. Variations in eastern North Pacific demersal fish biomass based on the U.S. west coast groundfish bottom trawl survey (2003–2010). Fish. B 110, 205–222.

Koslow, J.A., Goericke, R., Lara-Lopez, A., Watson, W., 2011. Impact of declining intermediate-water oxygen on deepwater fishes in the California Current. Mar. Ecol. Prog. Ser. 436, 207–218.

Koslow, J.A., Miller, E.F., McGowan, J.A., 2015. Dramatic declines in coastal and oceanic fish communities off California. Mar. Ecol. Prog. Ser. 538, 221–227.

Kroeker, K.J., Kordas, R.L., Crim, R., Hendriks, I.E., Ramajo, L., Singh, G.S., Duarte, C.M., Gattuso, J.P., 2013. Impacts of ocean acidification on marine organisms: quantifying sensitivities and interaction with warming. Glob. Change Biol. 19, 1884–1896.

Krumhansl, K.A., Scheibling, R.E., 2012. Production and fate of kelp detritus. Mar. Ecol. Progr. Ser. 467, 281–302.

Lange, C.B., Weinheimer, A.L., Reid, F.M., Tappa, E., Thunell, R.C., 2000. Response of siliceous microplankton from the Santa Barbara Basin to the 1997–98 El Niño event. Cal. Coop. Ocean. Fish. 41, 186–193.

Lebrato, M., Iglesias-Rodriguez, D., Feely, R.A., Greeley, D., Jones, D.O.B., Suarez-Bosche, N., Lampitt, R.S., Cartes, J.E., Green, D.R.H., Alker, B., 2010. Global contribution of echinoderms to the marine carbon cycle: CaCO_3 budget and benthic compartments. Ecol. Monogr. 80, 441–467.

Levin, L.A., Dayton, P.K., 2009. Ecological theory and continental margins: where shallow meets deep. Trends Ecol. Evol. 24, 606–617.

Levin, L.A., Liu, K.K., Emeis, K.C., Breitburg, D.L., Cloern, J., Deutsch, C., Giani, M., Goffart, A., Hofmann, E.E., Lachkar, Z., Limburg, K., Liu, S.M., Montes, E., Naqvi, W., Rague-neau, O., Rabouille, C., Sarkar, S.K., Swaney, D.P., Wassman, P., Wishner, K.F., 2015. Comparative biogeochemistry–ecosystem–human interactions on dynamic continental margins. J. Mar. Syst. 141, 3–17.

Lohrer, A.M., Thrush, S.F., Gibbs, M.M., 2004. Bioturbators enhance ecosystem function through complex biogeochemical interactions. Nature 431, 1092–1095.

Lohrer, A.M., Thrush, S.F., Hunt, L., Hancock, N., Lundquist, C., 2005. Rapid reworking of subtidal sediments by burrowing spatangoid urchins. J. Exp. Mar. Biol. Ecol. 321, 155–169.

Mantua, N.J., Hare, S.R., Zhang, Y., Wallace, J.M., Francis, R.C., 1997. A Pacific interdecadal climate oscillation with impacts on salmon production. Am. Meteorol. Soc. 78, 1069–1079.

McClatchie, S., Goericke, R., Cosgrove, R., Auad, G., Vetter, R., 2010. Oxygen in the Southern California Bight: multidecadal trends and implications for demersal fisheries. Geophys. Res. Lett. 37.

McGowan, J.A., Cayan, D.R., Dorman, L.M., 1998. Climate-ocean variability and ecosystem response in the northeast. Pac. Sci. 281, 210–217.

Miller, A.J., Song, H., Subramanian, A.C., 2015. The physical oceanographic environment during the CCE-LTER years: changes in climate and concepts. Deep-Sea Res 112 (Pt. II), 6–17.

Miller, E.E., Schiff, K., 2012. Descriptive trends in southern California bight demersal fish assemblages since 1994. Cal. Coop. Ocean. Fish. 53, 107–131.

Moffitt, S.E., Hill, T.M., Roopnarine, P.D., Kennett, J.P., 2015. Response of seafloor ecosystems to abrupt global climate change. Proc. Natl. Acad. Sci. USA 112, 4684–4689.

Nam, S., Kim, H.J., Send, U., 2011. Amplification of hypoxic and acidic events by La Niña conditions on the continental shelf off California. Geophys. Res. Lett. 38.

Nam, S., Takeshita, Y., Frieder, C.A., Martz, T., Ballard, J., 2015. Seasonal advection of Pacific Equatorial Water alters oxygen and pH in the Southern California Bight. J. Geophys. Res. 120, 5387–5399.

Netburn, A.N., Koslow, J.A., 2015. Dissolved oxygen as a constraint on daytime deep scattering layer depth in the southern California current ecosystem. Deep-Sea Res. Pt. I 104, 149–158.

Nichols, F.H., Cacchione, D.A., Drake, D.E., Thompson, J.K., 1989. Emergence of burrowing urchins from California continental shelf sediments—a response to alongshore current reversals? Estuar. Coast Shelf S29, 171–182.

Paine, R.T., 1966. Food web complexity and species diversity. Am. Nat. 100, 65–75.

Pan, T.-C.F., Applebaum, S.L., Manahan, D.T., 2015. Experiment ocean acidification alters the allocation of metabolic energy. Proc. Natl. Acad. Sci. USA 112, 4696–4701.

Parmesan, C., 2006. Ecological and evolutionary responses to recent climate change. Annu. Rev. Ecol. Evol. Syst. 37, 637–669.

Parnell, P.E., Miller, E.F., Lennert-Cody, C.E., Dayton, P.K., Carter, M.L., Stebbins, T.D., 2010. The response of giant kelp (Macrocystis pyrifera) in southern California to low-frequency climate forcing. Limnol. Oceanogr. 55, 2686–2702.

Paulmier, A., Ruiz-Pino, D., Garcon, V., 2011. CO_2 maximum in the oxygen minimum zone (OMZ). Biogeosciences 8, 239–252.

Pisut D.P. The distance chemosensory behavior of the sea urchin Lytechinus variegatus, Masters Thesis, Georgia Institute of Technology, 2004.

Portner, H.O., Langenbuch, M., Michaelidis, B., 2005. Synergistic effects of temperature extremes, hypoxia, and increases in CO_2 on marine animals: from Earth history to global change. J. Geophys. Res. 110.

Prince, E.D., Goodyear, C.P., 2006. Hypoxia-based habitat compression of tropical pelagic fishes. Fish. Oceanogr. 15, 451–464.

Ramajo, L., Pérez-León, E., Hendriks, I.E., Marbà, N., Krause-Jensen, D., Sejr, M.K., Blicher, M.E., Lagos, N.A., Olsen, Y.S., Duarte, C.M., 2016. Food supply confers calcifiers resistance to ocean acidification. Sci. Rep. 6, 19374.

Reimers, C.E., Lange, C.B., Tabak, M., Bernhard, J.M., 1990. Seasonal spillover and varve formation in the Santa-Barbara Basin, California. Limnol. Oceanogr. 35, 1577–1585.

Reum, J.C.P., Alin, S.R., Harvey, C.J., Bednaršek, N., Evans, W., Feely, R.A., Hales, B., Lucey, N., Prince, E.D., McElhany, P., Netwon, J., Sabine, C.L., 2016. Interpretation and design of ocean acidification experiments in upwelling systems in the context of carbonate chemistry co-variation with temperature and oxygen. ICES J. Mar. Sci 73, 582–595.

Seibel, B.A., 2011. Critical oxygen levels and metabolic suppression in oceanic oxygen minimum zones. The Journal of Experimental Biology 214, 326–336.

Sellanes, J., Neira, C., 2006. ENSO as a natural experiment to understand environmental control of meiofaunal community structure. Mar. Ecol 27, 31–43.

Send, U., Nam, S., 2012. Relaxation from upwelling: the effect on dissolved oxygen on the continental shelf. J. Geophys. Res. 117.

Somero, G.N., Beers, J.M., Chan, F., Hill, T.M., Klinger, T., Litvin, S.Y., 2016. What changes in the carbonate system, oxygen, and temperature portend for the northeastern Pacific ocean: a physiological perspective. BioScience 66, 14–26.

Stramma, L., Prince, E.D., Schmidtko, S., Luo, J.G., Hoolihan, J.P., Visbeck, M., Wallace, D.W.R., Brandt, P., Kortzinger, A., 2012. Expansion of oxygen minimum zones may reduce available habitat for tropical pelagic fishes. Nat. Clim. Change 2, 33–37.

Stumpp, M., Truebenbach, K., Brennecke, D., Hu, M.Y., Melzner, F., 2012. Resource allocation and extracellular acid-base status in the sea urchin Strongylocentrotus droebachiensis in response to CO_2 induced seawater acidification. Aquat. Toxicol. 110, 194–207.

Sydeman, W.J., Garcia-Reyes, M., Schoeman, D.S., Rykaczewski, R.R., Thompson, S.A., Black, B.A., Bograd, S.J., 2014. Climate change and wind intensification in coastal upwelling ecosystems. Science 345, 77–80.

Taylor, J.R., Lovera, C., Whaling, P.J., Buck, K.R., Pane, E.F., Barry, J.P., 2014. Physiological effects of environmental acidification in the deep-sea urchin Strongylocentrotus fragilis. Biogeosciences 11, 1413–1423.

Tegner, M.J., Dayton, P.K., 1987. El Niño effects on southern California kelp forest communities. Adv. Ecol. Res. 17, 243–279.

Thompson, B., Tsukada, D., Laughlin, J., 1993. Megabenthic assemblages of coastal shelves, slopes, and basins off southern California. Bull. South. Calif. Acad. Sci. 92, 25–42.

Thompson, B.E., Jones, G.F., 1987. Benthic macrofaunal assemblages of slope habitats in the southern California USA borderland. Allan Hancock Found. Occas., 1–21.

Thompson, B.E., Laughlin, J.D., Tsukada, D.T., 1983. Ingestion and oxygen consumption by slope echinoids. Annu. Rep. South. Calif. Coast. Water Res. Proj. 84, 93–107.

Thorsen, M.S., 1998. Microbial activity, oxygen status and fermentation in the gut of the irregular sea urchin Echinocardium cordatum (Spatangoida: Echinodermata). Mar. Biol. 132, 423–433.

Vetter, E.W., Dayton, P.K., 1998. Macrofaunal communities within and adjacent to a detritus-rich submarine canyon system. Deep-Sea Res 45 (Pt. II), 25–54..

Vopel, K., Vopel, A., Thistle, D., Hancock, N., 2007. Effects of spatangoid heart urchins on O_2 supply into coastal sediment. Mar. Ecol. Prog. Ser, 161–171.

Watts, S.A., McClintock, J.B., Lawrence, J.M., 2007. Ecology of Lytechinus. Dev. Aquac. Fish. Sci. 37, 473–497.

Wishner, K.F., Outram, D.M., Seibel, B.A., Daly, K.L., Williams, R.L., 2013. Zooplankton in the eastern tropical north Pacific: boundary effects of oxygen minimum zone expansion. Deep-Sea Res. 79 (Pt. I), 122–140.

Wolter, K., Timlin, M.S., 2011. El Niño/Southern Oscillation behaviour since 1871 as diagnosed in an extended multivariate ENSO index (MEI.ext). Int. J. Climatol. 31, 1074–1087.